Theor Chem Acc (2004) 111:1–17
DOI 10.1007/s00214-003-0505-8

Theoretical
Chemistry Accounts

Feature article

Correlation factor approach to the correlation energy functional

L. Pastor-Abia, A. Pérez-Jiménez, J. M. Pérez-Jordá, J. C. Sancho-García, E. San-Fabián, F. Moscardó

Departamento de Química Física, Universidad de Alicante, Apartado 99, 03080 Alicante, Spain

Received: 4 March 2003 / Accepted: 28 July 2003 /

Abstract. A global survey of the correlation factor energy functionals and its application to atomic and molecular properties is made. Its performances are compared with those of the density functional theory (DFT) correlation energy functionals, and some interesting conclusions from previous publications are reinforced here; namely, after removing the one-Slater-determinant hypothesis from the Kohn–Sham method, all DFT correlation functionals are able to provide reasonable results in any circumstance, with an additional restriction, for systems having a quasi-degenerate wave function, the DFT correlation functionals must depend explicitly on the on-top density.

Keywords: Correlation energy – Correlation factor – Density functional theory – Atomic properties – Molecular properties

1 Introduction

In this article, an overview of the application to atoms and molecules of two type of correlation energy functionals is made. One class is connected with the density functional theory (DFT); the other is obtained by factorization of the wave function or the two-body density matrix. The latter are the correlation factor (CF) methods also called two-body density (TBD) methods, to emphasize the difference with the DFT functionals, which are associated to the electronic density.

During the last few years, the impact of DFT on the quantum chemistry community has increased considerably, so nowadays the application of DFT to solve problems regarding reactivity as well as atomic and molecular structure is routine. Most of the DFT applications fall within the Kohn–Sham (KS) method, which has a practical implementation very similar to Hartree–Fock (HF) theory, although they have deep conceptual differences. With the aim of easing the following discussion, we will illustrate some key points.

HF theory consists of obtaining the Slater determinant which optimizes the expectation value of the electronic Hamiltonian:

$$E_{\mathrm{HF}} = \langle D|\hat{H}|D\rangle \ , \tag{1}$$

where D is a normalized Slater determinant:

$$D = (n!)^{-1/2}|\varphi_1(1)\cdots\varphi_n(n)| \ , \tag{2}$$

with φ_j being the jth spin-orbital and n the number of electrons.

The Born–Oppenheimer nonrelativistic electron Hamiltonian is, in atomic units,

$$\hat{H} = -\sum_{j=1}^{n}\frac{\Delta_j}{2} - \sum_{\alpha=1}^{m}\sum_{j=1}^{n}\frac{Z_\alpha}{|\mathbf{r}_j - \mathbf{R}_\alpha|} + \sum_{j>i=1}^{n}\frac{1}{|\mathbf{r}_j - \mathbf{r}_i|} \ , \tag{3}$$

where m is the number of nuclei and Z_α their corresponding charges.

In the HF theory, the optimum Slater determinant is obtained by iterating on the eigenvalue equations:

$$F^k|\phi_j\rangle = \varepsilon_j|\phi_j\rangle \ , \tag{4}$$

with

$$F^k = t + v + g_k \ , \tag{5}$$

where

$$t = -\frac{\Delta}{2} \ , \tag{6}$$

$$v = -\sum_{\alpha=1}^{m}\frac{Z_\alpha}{|\mathbf{r} - \mathbf{R}_\alpha|} \ , \tag{7}$$

and

$$g_k = a_k J_k - b_k K_k \ , \tag{8}$$

with

$$J_k = \sum_{j\in k}\int d\mathbf{r}'\,\frac{\phi_j^*(\mathbf{r}')\phi_j(\mathbf{r}')}{|\mathbf{r} - \mathbf{r}'|} \tag{9}$$

Correspondence to: F. Moscardó
e-mail: federico@fisic1.ua.es

and

$$K_k = \sum_{j\in k} \int d\mathbf{r}' \frac{\phi_j^*(\mathbf{r}')P(\mathbf{r},\mathbf{r}')\phi_j(\mathbf{r}')}{|\mathbf{r}-\mathbf{r}'|}\delta_{\sigma,\sigma'} \ , \tag{10}$$

where $P(\mathbf{r},\mathbf{r}')$ is the exchange operator between $\mathbf{r}$ and $\mathbf{r}'$ coordinates and σ and σ' are the spin indexes.

In the previous equations k runs over the different groups of orbitals.

The values of the a_k and b_k coefficients define the level into the HF theory (restricted (RHF), restricted open-shell (ROHF), unrestricted (UHF)).

We highlight the following key points into HF theory:

- It is a theory that, without further restrictions, gives an upper bound to the energy of the lowest state within each symmetry.
- This theory takes into account the Pauli principle, through the form selected for the wave function (Eq. 2).
- HF equations are nonlocal ones, owing to the exchange operator in Eq. (10).
- RHF theory is inadequate to study states that require more than one Slater determinant to correctly describe their wave function.
- HF theory is usually a good reference wave function to build better approximations to the exact wave function of a molecule.

The KS method supposes the existence of a Slater determinant built from spin-orbitals giving the exact density

$$\rho(\mathbf{r}) = \sum_j^n \left|\varphi_j^{\mathrm{KS}}\right|^2 \ . \tag{11}$$

The KS spin-orbitals fulfill the eigenvalue equations:

$$(t+v_{\mathrm{s}})\phi_j^{\mathrm{KS}} = \varepsilon_j \phi_j^{\mathrm{KS}} \ , \tag{12}$$

with

$$v_{\mathrm{s}} = v + v_{\mathrm{e}} + v_{\mathrm{xc}} \ , \tag{13}$$

where t and v (kinetic and external potential operators respectively) are defined by Eqs. (6) and (7). v_{e} is the repulsive electron-electron potential, similar to Eq. (9) but defined by the exact–density:

$$v_{\mathrm{e}} = \int \mathrm{d}\mathbf{r}' \frac{\rho(\mathbf{r}')}{|\mathbf{r}-\mathbf{r}'|} \ . \tag{14}$$

It is, as in Eq. (9), a local potential, but the difference is that this represents the exact Coulomb repulsion potential. The v_{xc} potential of Eq. (13) is the main difference from HF theory. The expression for this potential is unknown a priori, but it must incorporate all exchange and correlation effects. There are a lot of descriptions and discussions of KS theory [1], although there are some key points to be underlined:

- As in HF theory, KS is a method for the ground state of each symmetry.
- We could calculate the exact energy of a system, if we knew the exact functional for the energy, through the density obtained with the KS orbitals.
- The expression for the exchange–correlation potential of Eq. (13) can be obtained as the functional derivative of the exact exchange-correlation energy ($E_{\mathrm{xc}}[\rho]$):

$$v_{\mathrm{xc}}[\rho] = \frac{\delta E_{\mathrm{xc}}[\rho]}{\delta\rho} \ . \tag{15}$$

However, an important limitation of the KS method is that the exact expression of $E_{\mathrm{xc}}[\rho]$ is not known.

Usually the KS theory is assumed to be a local theory, having an effective local potential, although strictly this may not be so [2]. In fact, a lot of KS applications use a nonlocal effective potential, for example, when the exchange used includes the HF exchange, as in the hybrid exchange–correlation functionals.

In the next section, the characteristics of correlation functionals deduced from the CF approach will be exposed, emphasizing their approximations and limitations.

We will afterwards make the analysis of their performance on a wide variety of topics, either in a post-self-consistent-field (SCF) procedure, or in a SCF one. The behavior of these functionals used in post-SCF calculations is shown in Sect. 3 through a large variety of examples, comparing them with density functional results, so we begin with a discussion about their results on atomic and molecular properties, reactivity applications and excited-state calculations. SCF correlated calculations are dealt with in Sect. 4, and finally in Sect. 5, we discuss a method to solve the size-consistency problem that appears in some of the correlation energy functionals studied. Through these sections, several fundamental questions related to KS theory are discussed, such as the the use of a single-determinant wave function to obtain the exact density.

The last section is devoted to a global discussion about the most relevant results shown in this paper.

2 The CF approach

The paper by Colle and Salvetti (CS) [3] pioneered the systematic application of the CF approach to the calculation of the correlation energy. Since then, the expressions of CS have been used with success in a number of systems. One of the most popular and widespread used functionals within DFT, the Lee, Yang and Parr (LYP) functional [4] is a simplification of the CS equation when the two-body density matrix is that of a Slater determinant, leading to an expression which only depends on the charge density. The more than 7000 citations that either the functional or the model has received since it was published show the interest that it has created in the scientific community.

The key points of the CS model are are as follows.

The wave function is written within the CF approach [5, 6, 7] and for the correlated system is approximated in Ref. [3] as

$$\Psi(\mathbf{x}_1,\ldots,\mathbf{x}_n) = \Psi^0(\mathbf{x}_1,\ldots,\mathbf{x}_n)\Pi_{i<j}^n[1-\varphi(\mathbf{r}_i,\mathbf{r}_j)] \ , \tag{16}$$

where $\Psi^0(\mathbf{x}_1, \ldots, \mathbf{x}_n)$ is a reference wave function that in the first paper by CS [3] was chosen as a HF one, although in later papers it was extended to more elaborate multiconfigurational (MC) wave functions [8, 9, 10]. $\mathbf{x}_i$ represents both the spatial, $\mathbf{r}_i$, and spin, s_i, coordinates of electron i, while the CF, φ, is given by

$$\varphi(\mathbf{r}_1, \mathbf{r}_2) = \exp(-\beta^2 r^2)[1 - \Phi(\mathbf{R}_{12})(1 + r/2)] \ , \tag{17}$$

with $\mathbf{R}_{12} = (\mathbf{r}_1 + \mathbf{r}_2)/2$ and $r = |\mathbf{r}_1 - \mathbf{r}_2|$. $\Phi(\mathbf{R})$ plays an important role, since it governs the behavior of the model wave function at the correlation cusp ($r = 0$). β measures the inverse of the correlation radius, and according with Wigner's model it is

$$\beta = q\rho^{1/3} \ , \tag{18}$$

where q is a parameter optimized in Ref. [3] to the value of 2.29.

The mean value theorem is invoked to obtain an approximation to the two-body density. $\Phi(\mathbf{R}_{12})$ is approximated as

$$\Phi_{\mathrm{CS}}(\mathbf{R}) = \frac{\beta\pi^{1/2}}{1 + \beta\pi^{1/2}} \ . \tag{19}$$

The correlation energy functional is developed around the point $\mathbf{r} = 0$ in a Taylor series and truncated to second order. Further integration on $\mathbf{r}$ leads to a functional of the two-body density dependent on the $\mathbf{R}$ coordinates only. Finally, the resulting equation (Eq. 9 of Ref. [3]) is approximated by fitting its integrand by an approximate function parametrically adjusted (Eq. 19 of Ref. [3]).

Several deficiencies of the CS energy functional have been criticized [11, 12, 13, 14], all them related to the approximations taken in developing the correlation energy functional from Eq. (19) of Ref. [3]:

- The sum rule or equivalently

  $$\int \rho_{\mathrm{ch}}(\mathbf{r})\, \mathrm{d}\mathbf{r} = 0 \ , \tag{20}$$

  where $\rho_{\mathrm{ch}}(\mathbf{r})$ is the correlation hole, is not satisfied.
- The pair correlation energy density and the correlation potential are not well behaved [11, 12].
- The electron-gas correlation energy is not reproduced by the CS functional [13].
- The N-representability is lost in the CS procedure [14].

The Equation (20) for the coulomb hole density is not satisfied by the CS functional because Eq. (19) is used to write $\Phi(\mathbf{R})$, and Eq. (19) follows from integration of

$$\int \varphi(\mathbf{R}, \mathbf{r})\, \mathrm{d}\mathbf{r} = 0, \tag{21}$$

which is not related to any known physical constraint.

The deficiencies of the pair energy density are related to Eq. (19) of Ref. [3] and its parameterization. This equation is used instead Eq. (9) of Ref. [3] to avoid the divergences shown by it. A deeper question is the N-representability lost in the CS formulation because it is related to the way used in Ref. [3] to go from the N-body problem to the two-body one.

A procedure in the framework of the CF approach, different to that of CS, was proposed in Refs. [14, 15] and was aimed at solving the most important drawbacks of this model which were commented on earlier. Instead of starting from a wave function like that of Eq. (16), the exact second-order density matrix is taken as

$$\Gamma_2(\mathbf{r}_1, \mathbf{r}_2; \mathbf{r}'_1, \mathbf{r}'_2) = \Gamma^0_2(\mathbf{r}_1, \mathbf{r}_2; \mathbf{r}'_1, \mathbf{r}'_2)[1 + F(\mathbf{r}_1, \mathbf{r}_2; \mathbf{r}'_1, \mathbf{r}'_2)] \ , \tag{22}$$

where $\Gamma^0_2(\mathbf{r}_1, \mathbf{r}_2; \mathbf{r}'_1, \mathbf{r}'_2)$ is the spinless second-order density matrix corresponding to a model wave function, while $F(\mathbf{r}_1, \mathbf{r}_2; \mathbf{r}'_1, \mathbf{r}'_2)$ is a CF. The procedure that follows is described in detail in Ref. [14], and here we will only outline its most important issues.

We restrict $\Gamma_2(\mathbf{r}_1, \mathbf{r}_2; \mathbf{r}'_1, \mathbf{r}'_2)$ to be Hermitian, antisymmetric with respect to the exchange of the coordinates of two particles, and positive semidefinite:

$$\Gamma_2(\mathbf{r}_1, \mathbf{r}_2; \mathbf{r}'_1, \mathbf{r}'_2) = \Gamma^*_2(\mathbf{r}_1, \mathbf{r}_2; \mathbf{r}'_1, \mathbf{r}'_2) \tag{23}$$

$$\begin{aligned}\Gamma_2(\mathbf{r}_1, \mathbf{r}_2; \mathbf{r}'_1, \mathbf{r}'_2) &= -\Gamma_2(\mathbf{r}_2, \mathbf{r}_1; \mathbf{r}'_1, \mathbf{r}'_2) \\ &= \Gamma_2(\mathbf{r}_2, \mathbf{r}_1; \mathbf{r}'_2, \mathbf{r}'_1)\end{aligned} \tag{24}$$

$$\Gamma_2(\mathbf{r}_1, \mathbf{r}_2; \mathbf{r}'_1, \mathbf{r}'_2) \geq 0 \ . \tag{25}$$

These three are necessary, (but not sufficient), conditions for Γ_2 to be N-representable [16, 17]. An expression for the CF consistent with these requirements and close to the CS procedure is given by

$$\begin{aligned}F(\mathbf{r}_1, \mathbf{r}_2; \mathbf{r}'_1, \mathbf{r}'_2) &= \Lambda(\mathbf{r}_1, \mathbf{r}_2)\Lambda^*(\mathbf{r}'_1, \mathbf{r}'_2) \\ &\quad - \Lambda(\mathbf{r}_1, \mathbf{r}_2) - \Lambda^*(\mathbf{r}'_1, \mathbf{r}'_2)\end{aligned} \ , \tag{26}$$

with $\Lambda(\mathbf{r}_1, \mathbf{r}_2)$ being a function that does not depend on the angular components of r_{12},

$$\Lambda(\mathbf{r}_1, \mathbf{r}_2) = \Lambda(\mathbf{R}, r), \tag{27}$$

and chosen as

$$\Lambda(\mathbf{R}, r) = \exp[-\beta(\mathbf{R})r]^n[1 - \xi(\mathbf{R}, r)] \ , \tag{28}$$

where the value $n = 2$ which also appears in the CS formulation allows the analytical integration in the variable r. $\beta(\mathbf{R})$ is related to the exclusion radius of Wigner in the same manner as in the CS work. The $\xi(\mathbf{R}, r)$ function will be defined later.

A critical point in the CS model is that the Taylor expansion of $\Gamma^0_2(\mathbf{R}, r)$ around $r = 0$ is taken up to second order, which leads to undesired divergences in the correlation energy density. In order to avoid this problem a Gaussian summation was used in Ref. [14] to approximate $\Gamma^0_2(\mathbf{R}, r)$:

$$\Gamma^0_2(\mathbf{R}, r) = \Gamma^0_2(\mathbf{R})P(\mathbf{R}, r)\exp[-r^2/\gamma(\mathbf{R})], \tag{29}$$

where $\Gamma^0_2(\mathbf{R}) = \Gamma^0_2(\mathbf{R}, 0)$ and $P(\mathbf{R}, r)$ is a polynomial in r whose coefficients depend on $\gamma(\mathbf{R})$. Both $\gamma(\mathbf{R})$ and these coefficients will be fixed by means of some boundary conditions commented on later. Gaussian forms have been used previously to approximate the diagonal elements of density matrices with results that, in general, may be considered good [15, 18, 19]. Equation (29) was justified extensively in Ref. [18] where $\Gamma_2^0(\mathbf{R})$ was chosen to be that of one Slater determinant and $P(\mathbf{R},r)$ was taken to be constant and equal to 1. In this case $\Gamma_2^{\mathrm{det}}(\mathbf{R},\mathbf{r})$ takes the following form:

$$\begin{aligned}\Gamma_2^{\mathrm{det}}(\mathbf{R},\mathbf{r}) = {} & \frac{1}{2}\rho\left(\mathbf{R}+\frac{\mathbf{r}}{2}\right)\rho\left(\mathbf{R}-\frac{\mathbf{r}}{2}\right) \\ & -\frac{1}{2}\sum_{\sigma}\left[\rho_1^{\sigma\sigma}\left(\mathbf{R}+\frac{\mathbf{r}}{2};\mathbf{R}-\frac{\mathbf{r}}{2}\right)\right. \\ & \left.\times\,\rho_1^{\sigma\sigma}\left(\mathbf{R}-\frac{\mathbf{r}}{2};\mathbf{R}+\frac{\mathbf{r}}{2}\right)\right] \ , \qquad (30)\end{aligned}$$

where σ is the spin index, and ρ_1 is the first-order density matrix without spin.

If the orbitals that build ρ and ρ_1 are developed in a Taylor series the last equation may be written as

$$\Gamma_2^{\mathrm{det}}(\mathbf{R},\mathbf{r}) = \sum_k g_{2k}(\mathbf{R})r^{2k} \ . \qquad (31)$$

Therefore, a Gaussian form like that given by Eq. (29) with $P(\mathbf{R},r)=1$ is a good approximation to Eq. (31). The polynomial $P(\mathbf{R},r)$ was introduced in Ref. [14] to improve the model. On the other hand, the cusp condition on $\Gamma_2(\mathbf{R},r)$,

$$\left.\frac{\partial\Gamma_2(\mathbf{R},r)}{\partial r}\right|_{r=0} = \Gamma_2(\mathbf{R},0) \ , \qquad (32)$$

is used to model $F(\mathbf{R},r)$.

Taking the following form for $\xi(\mathbf{R},r)$

$$\xi(\mathbf{R},r) = \Phi(\mathbf{R})f(\mathbf{R},r) \qquad (33)$$

Eq. (32) transforms as

$$\left.\frac{\mathrm{d}}{\mathrm{d}r}f(\mathbf{R},r)\right|_{r=0} = \frac{1-a_1(\mathbf{R})}{2}f(\mathbf{R},0) \ , \qquad (34)$$

where $a_1(\mathbf{R})$ is the coefficient of order 1 in the polynomial $P(\mathbf{R},r)$. We note in the passing that if a_1 were zero we would end up with a condition for $f(\mathbf{R},r)$ consistent with the CS form, c.f. Eq. (17). Hence, Eq. (34) suggests two possible ways to define $f(\mathbf{R},r)$; namely,

$$f(\mathbf{R},r) = 1 + \frac{1-a_1(\mathbf{R})}{2}r + b_2r^2 \qquad (35)$$

or

$$f(\mathbf{R},r) = \exp(1-a_1(\mathbf{R}))r/2 \ , \qquad (36)$$

that would allow analytic integration in r.

The expression for $\Phi(\mathbf{R})$ is obtained from

$$\int \Gamma_2^0(\mathbf{R})[\Lambda(\mathbf{R},\mathbf{r})^2 - 2\cdot\Lambda(\mathbf{R},\mathbf{r})]\,\mathrm{d}\mathbf{R} = 0, \qquad (37)$$

which assumes that $\rho(\mathbf{r})=\rho^0(\mathbf{r})$. Finally, $\gamma(\mathbf{R})$, which enters in the Gaussian sum of Eq. (29), is obtained from the reducibility condition for $\Gamma_2^0(\mathbf{R},\mathbf{r})$ to $\omega^0(\mathbf{R})$ (the extracule density of the reference system):

$$\omega^0(\mathbf{R}) = \frac{8\pi}{N-1}\int_0^\infty r^2\Gamma_2^0(\mathbf{R},r)\,\mathrm{d}r \ . \qquad (38)$$

By using the set of equations (22–38) a set of correlation functionals depending on $\Gamma_2^0(\mathbf{R})$ was obtained in Refs. [14, 15]. The parameters entering through Eq. (35) or Eq. (36) together with q of Eq. (18) and the coefficients of $P(\mathbf{R},r)$ in Eq. (29) were obtained by fitting the exact correlation energies of the first-row atoms. From the set of correlation functionals of Refs. [14, 15] the Moscardó–San Fabián (MSF) functional [15] and the Moscardó–Pérez-Jiménez at level 5 (MPJ) of Ref. [14] were chosen. The first functional is obtained by assuming that $P(\mathbf{R},r)$ of Eq. (29) is a constant equal to 1. And the MPJ functional uses for $P(\mathbf{R},r)$ a polynomial of degree 2 and Eq. (35) to define $f(\mathbf{R},r)$.

In the next sections we discuss the results achieved by some of the correlation energy functionals. They are also compared with other correlation energy functionals presented in the literature. The comparison will be useful to overview the overall performance of functionals derived in the formalism of the CF approach, as well as to shed light on topics related to some known deficiencies found in the KS implementation of DFT.

3 Post-SCF calculations

In this section we show the capabilities of CS [3], MSF [15] and MPJ [14] correlation energy functionals applied in a post-SCF procedure. The total energy is evaluated as [20–24].

$$E_{\mathrm{A}}^f[\Psi_{\mathrm{A}}] = E_{\mathrm{A}}[\Psi_{\mathrm{A}}] + E_{\mathrm{c,A}}^f[\Psi_{\mathrm{A}}] \ , \qquad (39)$$

where Ψ_{A} indicates the class of wave function used (HF or MC) in the SCF evaluation of E_{A}, while f denotes the functional used to calculate the correlation energy, E_{c}.

Several authors have successfully applied this approach to approximate, in a post-SCF fashion, KS results in atoms and small molecules. These post-SCF–KS calculations can be justified because the contribution of the correlation potential, $\hat{v}_{\mathrm{c}}$, to the full effective KS Hamiltonian, Eq. (12), may be considered to be a small perturbation, (we will usually employ exact HF-type exchange). Under the assumption that the $\hat{v}_{\mathrm{c}}$ component of $\hat{v}_{\mathrm{xc}}$ is small compared with the rest of terms appearing in Eq. (13) we may take

$$\rho_\sigma^{\mathrm{KS}}(\mathbf{r}) \simeq \rho_\sigma^{\mathrm{HF}}(\mathbf{r}) \ , \qquad (40)$$

and hence

$$E_{\mathrm{KS}}[\rho_\sigma^{\mathrm{KS}}] \simeq E_{\mathrm{KS}}[\rho_\sigma^{\mathrm{HF}}] = E_{\mathrm{HF}} + E_{\mathrm{c}}[\rho_\sigma^{\mathrm{HF}}] \ . \qquad (41)$$

In the case of MC calculations, the use of the post-SCF scheme by Eq. (39) may be justified more easily from the perspective of the CF approach. Recall that since

$$\Gamma_2(\mathbf{r}_1,\mathbf{r}_2) = \Gamma_2^0(\mathbf{r}_1,\mathbf{r}_2) + \Delta\Gamma_2^0(\mathbf{r}_1,\mathbf{r}_2) \qquad (42)$$

the total energy may be partitioned as

$$E = E[\Gamma_2^0] + E[\Delta\Gamma_2^0] \ , \qquad (43)$$

where $E[\Delta\Gamma_2^0]$ defines the correlation energy of the partition. If the two members on the right-hand side of Eq. (43) are included in the SCF calculation, both Γ_2^0 and $\Delta\Gamma_2^0$ must be evaluated simultaneously. Nevertheless, as shown in Sect. 4, the contribution of $\Delta\Gamma_2^0$ to the SCF equations is quite small, and it is also a good approximation to take Γ_2^0 as that yielded by the the SCF evaluation of only $E[\Gamma_2^0]$.

3.1 Atomic properties

The first ionization potentials (IP) and electron affinities (EA) from post-HF and post-configuration interaction (CI) wave functions are shown and compared with those yielded by other well-known correlation energy functionals. We also discuss the accuracy of several sets of "exact" correlation energies that may be used as a reference to test the performance of correlation energy functionals. Finally, we comment on using several Slater determinants to calculate the total energy of some closed-shell isoelectronic series.

The exact nonrelativistic total energy, for each correlation energy functional, is approximated as

$$E^f(Z,N) = E_{\mathrm{HF}}(Z,N) + E_{\mathrm{c}}^f(Z,N) \ , \tag{44}$$

where f is the correlation energy functional employed in the calculation of the correlation energy, with N and Z being the number of electrons and the atomic number, respectively, of the atom, while E_{HF} is the energy of the HF wave function. The IP and EA are calculated using their definitions:

$$IP^f(Z) = E^f(Z,N-1) - E^f(Z,N) \ , \tag{45}$$

$$EA^f(Z) = E^f(Z,N) - E^f(Z,N+1) \ . \tag{46}$$

The results taken from Ref. [25] are for the atomic natural orbital–triple zeta (ANO-TZ) basis set [26, 27]. Although a high-quality basis set is not required to calculate E_{c} [28], it becomes essential to calculate E_{HF}, which is largely dependent on the basis set used.

The IP and EA values for several correlation energy functionals are shown in Tables 1 and 2. We have tested the CS, MSF and MPJ functionals as representative of CF ones, as well as some popular DFT correlation energy functionals, namely:

- The Vosko, Wilk and Nussair (VWN) [29] functional: a local spin density (LSD) correlation energy functional.
- The VWN functional with the self-interaction correction (SIC) of Ref. [20].
- The Perdew 86 [30] correlation energy functional, which is a representative functional of the generalized gradient approximation (GGA). We do not show the results of the popular LYP [4] correlation energy functional because this functional is a simplification of the CS functional when the wave function is approximated by a single Slater determinant. Hence, although the parameterization of the LYP functional is different to that of CS one, both functionals give very similar results.

Table 1. Ionization potentials (IP) (eV) obtained in a post-self-consistent-field (SCF) procedure

Z	Exact[a]	UHF	VWN	VWN-SIC	P86	CS	MSF	MPJ
2	24.59	23.45	25.72	25.04	24.70	24.58	24.53	24.59
3	5.39	5.34	5.78	5.39	5.54	5.55	5.67	5.66
4	9.32	8.04	9.43	8.99	9.09	8.90	9.04	8.95
5	8.30	8.04	9.02	8.43	8.67	8.53	8.55	8.56
6	11.26	10.80	11.84	11.18	11.52	11.36	11.27	11.31
7	14.53	13.90	14.97	14.26	14.68	14.48	14.31	14.37
8	13.62	12.02	13.97	13.31	13.47	13.24	13.58	13.69
9	17.42	15.65	17.53	16.82	17.05	16.85	17.09	17.21
10	21.56	19.71	21.54	20.77	21.07	20.88	21.03	21.15
11	5.14	0.11	5.43	5.04	5.17	5.25	5.16	5.22
12	7.65	6.61	7.84	7.42	7.56	7.42	7.56	7.52
13	5.99	5.61	6.40	5.89	6.24	5.94	5.98	6.03
14	8.15	7.64	8.50	7.95	8.35	8.04	8.03	8.10
15	10.49	9.91	10.83	10.23	10.68	10.36	10.30	10.39
16	10.36	9.24	10.83	10.27	10.54	10.27	10.57	10.68
17	12.97	11.76	13.36	12.75	13.08	12.80	13.05	13.18
18	15.76	14.56	16.15	15.50	15.88	15.58	15.78	15.93
ϵ		7.32	3.86	2.04	1.91	1.91	1.49	1.68

[a] Refs. [31, 32]

Table 2. Electron affinities (EA) (eV) obtained in a post-SCF procedure

Z	Exact[a]	UHF	VWN	VWN-SIC	P86	CS	MSF	MPJ
3	0.62	−0.12	0.74	0.50	0.61	0.38	0.51	0.41
5	0.28	−0.31	0.37	−0.08	0.26	−0.01	0.02	0.03
6	1.27	0.45	1.25	0.71	1.12	0.85	0.78	0.81
8	1.47	−0.58	0.94	0.39	0.62	0.42	0.63	0.71
9	3.41	1.18	2.70	2.08	2.36	2.19	2.31	2.41
11	0.55	−0.11	0.70	0.46	0.58	0.37	0.52	0.47
13	0.45	0.01	0.56	0.18	0.51	0.20	0.26	0.31
14	1.40	0.85	1.53	1.06	1.46	1.12	1.14	1.20
15	0.76	−0.33	0.96	0.53	0.76	0.52	0.77	0.80
16	2.09	0.88	2.22	1.73	2.02	1.76	1.98	2.04
17	3.64	2.37	3.73	3.18	3.53	3.25	3.43	3.52
ϵ		110.50	24.57	45.37	15.68	43.47	31.09	31.14

[a] Ref. [33]

The exact nonrelativistic IP values of Table 1 are taken from Davidson and coworkers [31, 32]. The exact EA nonrelativistic values listed in Table 2 correspond to the experimental values of Hotop and Lineberger [33] modified with the relativistic corrections of García de la Vega [34]. These tables also give the relative average errors of each functional calculated by the formula.

$$\epsilon^f(X) = \frac{100}{n}\sum_{Z}^{n}\frac{|X^f(Z) - X^{\mathrm{e}}(Z)|}{X^{\mathrm{e}}(Z)} \ , \tag{47}$$

where $X^f(Z)$ is the value of the IP or EA for the atom of atomic number Z calculated with the functional f and $X^{\mathrm{e}}(Z)$ is the exact value of the IP or EA for the atom of atomic number Z.

The relative average errors separate the functionals into two groups: the LSD functionals on one side and the LSD–SIC, GGA and CF ones on the other. As expected, the errors for the IP are lower than those for the EA results. However, the fraction $\frac{\epsilon^f}{\epsilon_{\mathrm{HF}}}$ is very similar for the IP compared to that of the EA. This means that adding the correlation energy notably improves the EA values.

3.1.1 Exact correlation energies

The calculated correlation energies were compared with two sets of “exact” values. Both sets are obtained by applying the expression

$$E_c(Z) = AE(Z) - E_{\mathrm{rel}}(Z) - E_{\mathrm{HF}}(Z) - E_{\mathrm{Lamb}}(Z) \ , \qquad (48)$$

where $AE(Z)$ is either the sum of the IPs of the atom with atomic number Z taken from Moore’s tables (we name this set of correlation energies A), or from the experimental energies given by Veillard and Clementi (named set B). E_{rel} and E_{HF} are the relativistic and limit HF energies, respectively, taken from Fraga and coworkers [35, 36], while E_{Lamb} is the Lamb displacement, whose calculation is discussed thoroughly in Refs. [14, 25]. The values of the correlation energies of sets A and B were taken from Ref. [25].

There is some uncertainty in the experimental determination of the innermost IP [31, 32] that gives an inaccuracy of 0.1 hartree in the correlation energy of second-row atoms. In the following we show that correlation energy functionals may aid in the validation of “exact” correlation energy sets.

The average error when evaluating the correlation energy by means of Eq. (44) with several correlation energy functionals is plotted in Fig. 1. We represent separately the average error with respect to the atoms of the first row from that referred to those of the second row for each set of exact values (named A and B) and each functional. The curves corresponding to the atoms of the first row are very similar, indicating the agreement between the “exact” correlation energies from both sets. We note in passing that while LSD and LSD–SIC functionals provide large errors, those corresponding to GGA and CF functionals are rather small. Regarding the results of the second row, the curve referring to set A is very different from that corresponding to set B of “exact” correlation energies. Unlike curve A, which shows both large average errors and a large dispersion, curve B approaches a straight line of zero slope with small average errors. This result suggests that the “exact” correlation energies of set B are good approximations to the correct values.

3.1.2 Two- and four-isoelectronic series

The calculations of the correlation energy for the two- and four-isoelectronic series shows some interesting features. For the two-isoelectronic series one Slater determinant built from the $1s$ orbital suffices to give a correct description of the systems. For the four-electron series, however, the interaction of the $2p$ orbitals with the $2s$ orbital is more important, increasing with Z. As a result, the $2p$ orbitals play an important role in the approximate wave-function to be used to obtain the correlation energy. With this fact in mind a CI wave function containing configurations $1s^2 2s^2$ and $1s^2 2p_q^2$ ($q = x, y, z$) was built, from which we calculated the correlation energy using CS and MSF functionals. These values, (together with the results using a RHF wave function), are depicted in Fig. 2 and recover the correct trend when compared with those obtained using a HF wave function as a reference. It is the first example of the role that the correct choice of the model of the wave function used plays to calculate the correlation energy.

3.2 Molecular properties

3.2.1 Diatomic Molecules

In this section we briefly comment on the most relevant results obtained when applying CF-type correlation functionals to the post-SCF evaluation of properties in diatomic molecules. We also compare these results with those provided by DFT functionals.

The values of the spectroscopic constants R_e equilibrium distance, vibrational frequency, ω_e, and dissociation energy, D_e, corresponding to the ground state of a set of heterodiatomic and homodiatomic molecules built from first-row atoms are reported in Table 3. Together with the exact results, we list those obtained from UHF

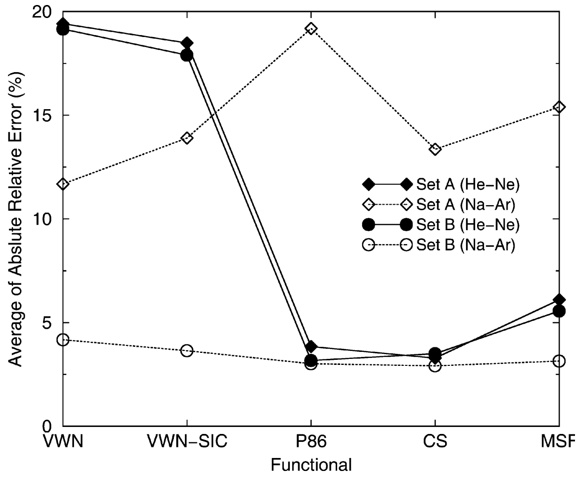

Fig. 1. Average of absolute relative errors for several correlation energy functionals

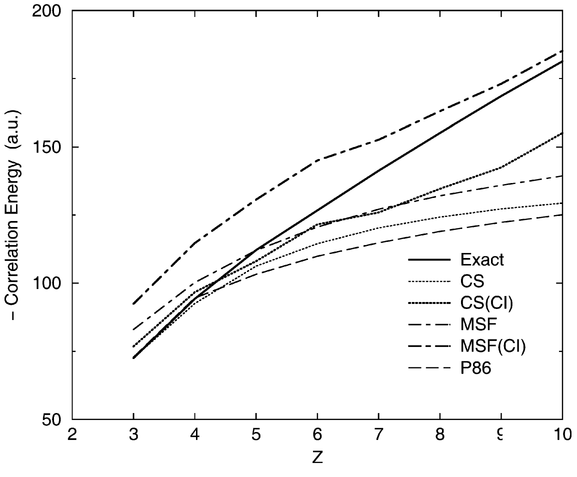

Fig. 2. Correlation energy for the four-isoelectronic series. In a.u.

Table 3. Equilibrium distance, R_e (au), dissociation energy, D_e (eV) and bond vibrational frequency, ω_e (cm^{-1}), calculated in a post-SCF procedure

	H_2	LiH	BH	FH	Li_2	C_2	N_2	F_2
Experimental								
R_e	1.401	3.015	2.336	1.733	5.051	2.347	2.073	2.679
D_e	4.75	2.52	3.58	6.12	1.14	6.36	9.91	1.66
ω_e	4400	1406	2368	4139	351	1855	2358	892
UHF								
R_e	1.390	3.038	2.314	1.693	5.538			
D_e	3.62	1.47	2.65	4.09	0.20			
ω_e	4581	1428	2470	4498	229			
UHF + VWN								
R_e	1.377	3.002	2.293	1.685	4.914			
D_e	4.95	2.60	3.66	5.14	0.84			
ω_e	4655	1466	2530	4554	413			
UHF + P86								
R_e	1.386	2.996	2.301	1.680	4.968			
D_e	4.75	2.46	3.61	5.42	0.82			
ω_e	4626	1471	2522	4609	393			
UHF + CS								
R_e	1.382	2.973	2.285	1.684	4.891			
D_e	4.64	2.38	3.53	5.16	0.75			
ω_e	4626	1492	2548	4566	402			
UHF + MSF								
R_e	1.380	3.000	2.290	1.684	4.941			
D_e	4.54	2.47	3.67	5.25	0.76			
ω_e	4647	1470	2541	4566	400			
GVB-PP								
R_e	1.430	3.093	2.370	1.728	5.537	2.443	2.079	2.873
D_e	4.12	1.92	3.15	4.81	0.44	2.84	7.10	0.55
ω_e	4208	1301	2260	4132	273	1548	2384	543
GVB + VWN								
R_e	1.416	3.052	2.347	1.718	5.412	2.425	2.066	2.831
D_e	4.28	2.11	3.31	5.03	0.52	3.19	7.83	0.62
ω_e	4299	1347	2322	4194	293	1587	2439	577
GVB + P86								
R_e	1.424	3.043	2.354	1.710	5.377	2.413	2.067	2.700
D_e	4.48	2.24	3.53	5.58	0.65	3.67	8.13	1.11
ω_e	4274	1356	2322	4278	299	1624	2439	733
GVB + CS								
R_e	1.413	2.987	2.344	1.708	5.096	2.348	2.007	2.704
D_e	4.74	2.59	3.93	6.25	0.94	6.89	12.34	2.48
ω_e	4380	1452	2302	4325	361	1830	2783	809
GVB + MSF								
R_e	1.411	3.028	2.330	1.708	5.230	2.397	2.051	2.753
D_e	4.79	2.66	3.91	5.88	0.91	5.64	10.64	1.46
ω_e	4368	1406	2359	4306	337	1679	2547	757

calculations, Generalized valence bond perfect pair (GVB-PP) [37, 38, 39] ones, and the corresponding post-SCF calculations derived from these two after adding the correlation energy (Eq. 39). Details about the basis sets used and the SCF calculations may be found in Ref. [40]. First of all, neither the UHF nor the GVB-PP wave functions can describe correctly the ground state of C_2 and N_2, and for this reason a minimal MC wave function was used for these two molecules. Secondly, the UHF results corresponding to the F_2 molecule are not shown because this potential-energy curve (PEC) is dissociative. Third, the GVB-PP data corresponding to the B_2 molecule are not given since it is not possible to correctly describe the valence electrons for it.

Regarding the post-UHF results we remark the following facts. As expected, adding the correlation always improves on the UHF values of D_e. This improvement is dramatic in some cases, such as in H_2, LiH or BH; however, deviations with respect to the exact values are still large for FH and B_2. For this type of wave function, all the functionals yield similar results. The correlation correction decreases the equilibrium distances and increases the vibrational frequencies. This trend results in a worsening of the correlated results since the UHF equilibrium distances (frequencies) are already shorter (larger) than the exact values. Pople [41] also reports a decrease of about 0.02–0.04 au in the equilibrium distance for UHF/6-31G* calculations. The correlation effect on these properties can be understood from the analysis performed in Ref. [40], where it was shown that the following equation holds between the equilibrium distance of the post-SCF correlated calculation, R_e^c, and that of the original SCF one, R_e:

$$\frac{1}{R_e^c} - \frac{1}{R_e} = \frac{\epsilon'_c}{\mu\omega_e^2 R_e^2} \quad , \tag{49}$$

while the following ones relate ω_e^c with ω_e: and D_e with D_e^c:

$$\omega_e^c = \omega_e \left(\frac{R_e}{R_e^c}\right) \quad , \tag{50}$$

$$D_e^c = D_e - \Delta\epsilon_c + \frac{\epsilon_c'^2}{2\mu\omega_e^2} \quad , \tag{51}$$

where μ is the reduced mass, ω_e^c and D_e^c are the values of the spectroscopic constants corresponding to the correlated post-SCF calculation, and where

$$\epsilon'_c = \left.\frac{dE_c(R)}{dR}\right|_{R=R_e} \tag{52}$$

and

$$\Delta\epsilon_c = E_c(R_e) - \lim_{R\to\infty} E_c(R) . \tag{53}$$

The trends mentioned are the result of $\epsilon'_c > 0$ and $\Delta\epsilon_c < 0$ in all the molecules analyzed.

Regarding to the post-GVB-PP calculations an increase in the dissociation energies compared to the original GVB-PP ones can be observed. On the other hand, this increment is larger for CF functionals than for DFT ones. This is due to the fact that DFT functionals, when added to the GVB-PP energy, tend to overestimate the energy of the quasi-dissociated molecule. However, the values of D_e obtained from post-GVB-PP calculations are better than those provided by the GVB-PP ones regardless of the functional used. As was also the case with the post-UHF calculations, the post-GVB-PP equilibrium distances decrease while the vibrational frequencies increase with respect to the GVB-PP results. This can be justified in the same way as done previously for the post-UHF calculations: see Eqs. (49–53).

Finally, we stress the fact that the best values of R_e, ω_e and D_e are given by the post-SCF calculations using a multideterminant wave function (GVB or MC). For this type of calculation it is also evident that CS or MSF functionals provide better results than those yielded by DFT ones.

3.2.2 The double count of the correlation energy

A problem which happens when calculating the correlation energy by means of correlation functionals is the so-called double count of the correlation energy. If the functional was well adapted to the wave function leading to the "uncorrelated" energy, then this kind of problem should not appear, and the correlation energy evaluated with respect to any reference wave function should automatically adjust its value. As a matter of example consider the ground state of the He atom: if the correlation functional was adapted to the wave function, the functional should give a correlation energy of −0.042 au when the reference wave function is a HF one, while it should provide no correlation energy at all if the reference wave function is a full CI one. However, most of the correlation functionals give an excess of correlation energy when the reference wave function includes more than a single Slater determinant; this excess of correlation energy is termed the double count of correlation energy. The post-GVB-PP and post-MC results discussed earlier obtained by using the DFT functionals suffer from this deficiency. The CF ones also suffer of the same deficiency, but to a lesser extent. This fact explains the better values obtained with the latter.

The effect of the wave function on the double count of the correlation energy has been studied in post-SCF calculations for a set of first row atoms and for PECs of diatomic molecules (H_2 and LiH) [42]. The reference wave functions used were HF, GVB-PP and CI with doubles (CID) and singles and doubles (CISD) with different excitation windows. The results shown in Table 4 for H_2 indicate that DFT functionals are not sensitive to the class of wave function used. As the wave function complexity increases the double count of the correlation energy also increases. In contrast, the CF functionals adequately modify the correlation energy they provide depending on the reference wave function used. A consequence is the quality of properties such as the frequencies for vibrational excited states (see Table 9 of Ref. [42]) for the post-SCF calculations compared with the frequencies obtained by Kolos and Wolniewicz [43].

A procedure has been proposed to cure the double count of the correlation energy in DFT functionals [44]. It consists of including the on-top two-body density matrix, $\rho_2(\mathbf{r},\mathbf{r}) \equiv \rho_2(\mathbf{r})$, in the expression of the DFT functional through

$$\rho = \rho'_\alpha + \rho'_\beta \ , \tag{54}$$

$$\rho'_{\alpha(\beta)} = \rho_{\alpha(\beta)} \pm \sqrt{\frac{\rho^2 - 2\rho_2}{2}} \ , \tag{55}$$

where ρ and ρ_2 are, respectively, the charge density and the on-top density of the multi-determinant wave function and ρ'_α and ρ'_β substitute the spin density components ρ_α and ρ_β (see Ref. [44] for the justification of these equations).

Equations (44) and (45) have also been used in the calculation of exchange energies [45], but the results are not as good as those obtained for the correlation, probably because the approximation that leads to them is not as accurate for exchange as for correlation. The use of Eqs. (54) and (55) in the post-GVB-PP and post-MC calculation of PECs of diatomic molecules, reaction energies and torsional barriers has proved to be an excellent method to remove the double count of the correlation energy [42]. As an example, the PEC corresponding to the ground state of H_2 evaluated in a post-SCF fashion with different combinations of wave functions and functionals is plotted in Fig. 3. The term P86m used in Fig. 3 refers to the P86 functional evaluated with the spin components given by Eqs. (54) and (55).

It is well known that a bad description of the dissociation is provided by RHF theory, as well as that this may be corrected if enough determinants are included in the wave function. For example, in Fig. 3 we can see that including the correlation energy does not modify significantly the wrong tendency of the RHF calculation. The correlation energy yielded by the CF functional when added to the GVB-PP calculation seems to incorporate the dynamic correlation lacking, improving the whole range of internuclear distances. When the P86 correlation energy is added to the GVB-PP the result is a translation of the GVB-PP curve. Nevertheless, the curve corresponding to the GVB-PP + P86m calculation recovers the correct shape of the GVB-PP + CFPEC. The slight difference between these two curves is due to

Table 4. Correlation energies for the hydrogen molecule

Method	R = 1.401 au				R = 10.0 au			
	HF	CISD		GVB	HF	CISD		GVB
		(1–2)	(1–12)			(1–2)	(1–12)	
SCF	0.0000	0.0015	0.0359	0.0184	−0.2357[a]	−0.0233[a]	0.0000[a]	0.0000[a]
VWN	0.0492	0.0491	0.0493	0.0493	0.0395	0.0396	0.0429	0.0429
P86	0.0472	0.0471	0.0471	0.0471	0.0333	0.0334	0.0337	0.0337
B88	0.0358	0.0358	0.0363	0.0361	0.0244	0.0245	0.0272	0.0272
LYP	0.0382	0.0381	0.0381	0.0381	0.0264	0.0264	0.0271	0.0271
CS	0.0376	0.0363	0.0021	0.0227	0.0289	0.0000	0.0000	0.0000
MSF	0.0338	0.0330	0.0062	0.0246	0.0266	0.0000	0.0000	0.0000
Exp.	0.041				0.000			

[a] $E_{\mathrm{SCF}}(H_2) - 2E_{\mathrm{HF}}(H)$

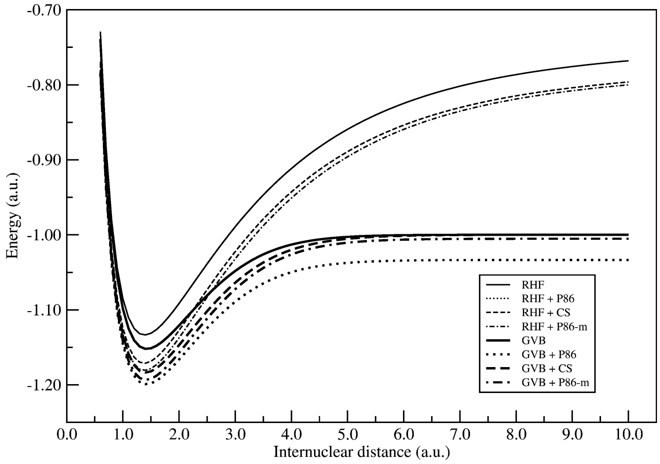

Fig. 3. Post-SCF potential energy curves of H_2 molecule. In a.u.

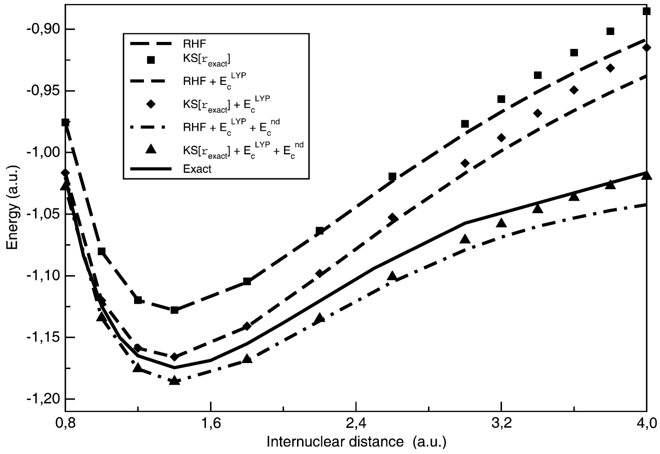

Fig. 4. Potential energy curves of H_2 molecule using the 6-311G** basis set. In a.u.

the residual autocorrelation energy of P86 for the hydrogen atom (−0.0024 au). It is specially remarkable that this lowering in the double count is produced to the correct extent along the whole PEC.

3.2.3 Beyond KS DFT

CF functionals may shed light on unsolved questions related to the KS implementation of DFT. One of these questions is the following: can the results obtained from the KS method be considered as parallel to those obtained from the HF method or, on the contrary, are they markedly different because KS and HF are theories of a totally different nature?

In the first case, KS results should reproduce the essential characteristics of HF ones. In other words the KS method should fail in the same cases where the HF method does. It is a well-known fact that the RHF method provides erroneous dissociative curves. On the other hand, the UHF method may yield the correct trend of the energy at dissociation distances but with fragments having fractional charges (as an example, the UHF solution corresponding to a dissociated Li_2^+ cation provides Li ions with $+1/2$ net charge) and wave functions that are not eigenfunctions of the $\hat{S}^2$ operator. These same behaviors have been found in restricted KS and unrestricted KS calculations using exact exchange and a lot of correlation energy functionals, and thus seem to confirm the first hypothesis.

Regarding the second possibility, it has been argued that the exact exchange–correlation functional evaluated with the exact density must contain all the information necessary to yield the exact value of the energy. If one is consistent with this for an even number of electrons, the exact density ρ_{exact} should take the following form:

$$\rho_{\mathrm{exact}}(\mathbf{r}) = \sum_{i=1}^{n} 2 \cdot \phi_i^{\mathrm{KS}^*}(\mathbf{r})\phi_i^{\mathrm{KS}}(\mathbf{r}) \ , \tag{56}$$

where $\phi_i^{\mathrm{KS}}(\mathbf{r})$ is a KS orbital solution of Eq. (12).

This closed-shell solution must be valid in the whole range of interatomic distances for the PEC of a diatomic molecule. The PEC for H_2 is plotted in Fig. 4 (another example and the details of the calculations can be seen in Ref. [46]). The points labeled $\mathrm{KS}[\rho_{\mathrm{exact}}]$ correspond to KS exchange-only energies using exact exchange (see Eq. 10) and the exact density, those labeled $\mathrm{KS}[\rho_{\mathrm{exact}}] + E_{\mathrm{c}}^{\mathrm{LYP}}$ are obtained from the former by adding the LYP correlation energy evaluated also with the exact density, and those labeled $\mathrm{KS}[\rho_{\mathrm{exact}}] + E_{\mathrm{c}}^{\mathrm{LYP}} + E_{\mathrm{c}}^{\mathrm{nd}}$ are calculated from the latter by adding an estimate of the nondynamic correlation energy following Mok et al. [47], namely

$$E_{\mathrm{c}}^{\mathrm{nd}} = E_{\mathrm{CASSCF}(n,m)} - E_{\mathrm{HF}} \ , \tag{57}$$

where n and m indicate the corresponding excitation window. The points whose label starts with RHF were obtained in the same fashion as those just described, but were evaluated self-consistently with the RHF orbitals and density.

The conclusions that can be drawn from this figure are clear. First of all, the use of either the HF density or the exact density in exchange-only KS calculations has almost no effect, apart from the slight increase of the energy in the case where the exact density is employed, which is in complete agreement with the variational principle. Secondly, when the correlation energy is included via a correlation energy functional, the PEC is almost parallel to the noncorrelated one regardless of the density (HF or exact) employed in the calculations. However, once the non-dynamical contribution is considered in the way described earlier the results lie much closer to those corresponding to the exact PEC. Therefore, it seems that the problems regarding the KS method have to do with the nondynamical correlation contribution. It could be argued that the DFT correlation energy functionals proposed in the literature are designed to only account for the dynamic contribution to correlation energy. If this were the case, the possibility of including the nondynamical contribution in them still remains. But Fig. 4 indicates that invoking such modification is unnecessary since DFT correlation energy functionals are able to yield excellent results without changing their expressions, but merely incorporating a dependence in the wave function through the on-top pair density.

3.3 Chemical reactivity

Although we have already shown that DFT performs quite well when dealing with properties of molecules near their equilibrium geometries, we now face a much more demanding problem, which is also of primary importance in chemistry; namely, the determination of reaction energies and activation barriers of chemical reactions.

3.3.1 Reaction energies

Apart from their interest as prototype reactions of interstellar chemistry, the following reactions are of particular interest to analyze the applicability of correlation energy functionals to chemical reactivity because the changes in the ionicity of the species represent a good test for them.

$$O^+(^4S) + H_2(^1\Sigma_g^+) \longrightarrow OH^-(^3\Sigma^-) + H(^2S) \tag{58}$$

$$OH^+(^1\Sigma^-) \longrightarrow O(^3P) + H^+ \tag{59}$$

$$OH^+(^1\Sigma^-) \longrightarrow O^+(^4S) + H(^2S)\ . \tag{60}$$

The results from Ref. [48] are listed in Table 5 for the spectroscopic constants of the $OH^+(^3\Sigma)$ molecule, the reaction energies for the reactions in Eqs. (58), (59) and (60) yielded by DFT and CF functionals, together with the experimental results and the results from multi-reference CI perturbation theory to second order (MRCI-MP2) calculations [49].

Regarding the functionals analyzed, we focus on P86 [30] and Becke (B88) [50] density functionals, as well as on MSF [15] and MPJ [14]. Results employing both a ROHF wave function and a GVB-PP one are shown. The calculations labeled P86m and B88m were done including a dependence on $\rho_2(\mathbf{r})$ through Eqs. (54) and (55). Also included are results from KS calculations [51] performed with Becke's exchange [52], together with either P86 (B-P86) [30] or LYP correlation energy functionals [4] (B-LYP), as well as with different proportions of HF exchange (B3-LYP [53]). All the values listed were obtained with the ANO-TZ basis set [26, 27].

The results indicate that inclusion of dynamic correlation by means of correlation energy functionals largely improves the results achieved by ROHF or GVB wave functions. When both dynamic and nondynamic contributions to the correlation energy are considered, the values of ΔE for Eq. (58) improve to a great extent. Regarding this, the improvement observed in P86 and B88 functionals is due to a lowering of ΔE, while for MSF and MPJ functionals the improvement comes from an increase of ΔE. KS calculations overestimate ΔE mainly because of Becke's exchange. Both MSF and MPJ functionals provide the best values. Actually, the MSF(GVB) calculation yields $\Delta E = -0.41\,\text{eV}$, with a relative error of -8.7% while the much more computationally demanding MRCI-MP2 calculations using as many as 1,512,109 configurations provides a large error of -33.3%.

Table 5. Molecular properties of OH^+

Method	R_e (au)	D_e (eV)[a]	D_e (eV)[b]	ΔE (eV)[c]
HF	1.900	3.54	5.16	0.10
P86	1.883	5.04	5.18	−0.12
B88	1.885	4.72	5.22	−0.10
MSF	1.888	5.14	5.16	−0.58
MPJ	1.883	5.26	5.18	−0.68
GVB	1.937	4.12	5.77	0.02
P86m	1.913	5.49	5.67	−0.23
B88m	1.913	5.11	5.62	−0.22
MSF	1.918	5.18	5.23	−0.41
MPJ	1.915	5.30	5.24	−0.50
BLYP	1.982	5.66	5.10	−1.03
BP86	1.977	5.83	5.20	−0.97
B3LYP	1.958	5.66	5.11	−0.88
Reference [49]	1.942	4.99	5.16	−0.30
Experiment[d]	1.944	5.21	5.20	−0.45 ± 0.002

[a] Dissociation energy of Eq. (60): $OH^+ \rightarrow O^+ + H$

[b] Dissociation energy of Eq. (59): $OH^+ \rightarrow O + H^+$

[c] Energy change in reaction of Eq. (58): $O^+ + H_2 \rightarrow OH^- + H$

[d] The result for ΔE is from Ref. [77], the rest are from Ref. [78]

3.3.2 Energy barriers

The automerization reaction of cyclobutadiene consists in the inter-conversion between two rectangular structures of D_{2h} symmetry through a square transition state of D_{4h} symmetry. Cyclobutadiene is an antiaromatic molecule and is exceedingly unstable, which makes it difficult to study experimentally. For this reason, much attention has been devoted to both the geometry of the molecule and the automerization mechanism by experimental [54] as well as by theoretical chemists [55, 56, 57]. From the theoretical point of view, this automerization reaction has difficulties rooted in the strong differences between the electronic structures of the rectangular and the square geometries. The ground state of cyclobutadiene is a singlet that can be conveniently represented by a single Slater determinant. On the other hand, the highest occupied level in the square geometry corresponds to two degenerate $\pi(e_g)$ orbitals housing two electrons. This implies that at least two Slater determinants are needed to qualitatively describe the square geometry of the transition state. The different character of the electronic structures of the D_{2h} and D_{4h} conformations requires well-balanced calculations to account for the automerization process. This can be achieved by multi reference calculations with a large excitation window. In this sense, multi reference coupled cluster (MR-CC) calculations have demonstrated their adequacy to handle this problem [56, 57]. Here we address it by means of post-SCF calculations performed with a wide range of DFT and CF correlation functionals, comparing their estimations for the automerization barrier with those provided by a very elaborate MR-CC calculation.

The automerization energy barriers obtained with the aforementioned correlation energy functionals and two types of wave functions are listed in Table 6: HF for a single-reference and GVB-PP for a two-reference wave function, respectively [46, 58]; the DFT was modified according to Eqs. (54) and (55) whenever the GVB-PP wave function was used.

Table 6. Automerization barrier (kcal/mol) of cyclobutadiene

Method	ΔE^{a}	ΔE^{b}	ΔE^{c}	ΔE^{d}	ΔE^{e}
HF	30.2	29.8			
LYP	29.7	29.4			
P86	29.3	29.1			
MSF	30.0	29.8			
MPJ	30.0	29.7			
GVB	11.0	11.5			
P86m	11.1	11.7	5.0	5.7	5.7
B88m	11.9	12.3	6.9	7.6	7.5
CS			5.3	6.0	6.1
MSF	12.8	13.0	7.7	8.4	8.4
MPJ	12.9	13.4	8.0	8.7	8.6
BLYP	25.4	22.6			
B3LYP	25.3	25.3			
Reference	6.4	7.0	6.4	7.0	7.4

[a] Using the cc-PVDZ basis set
[b] Using the cc-PVTZ basis set
[c] Using the cc-PVDZ basis set and Eq. (61)
[d] Using the cc-PVTZ basis set and Eq. (61)
[e] Using correlation energies extrapolated to the basis set limit

Two set of values, corresponding to a single-determinant and a two-determinant wave function, respectively, are reported. While the former is 5 times larger than the reference barrier, the latter is almost double it. This reveals the need of including the many-determinant character of the D_{4h} conformer, accounting for the correct description of the nondynamic correlation. However, if the D_{2h} conformer is described by a GVB-PP wave function, part of the residual dynamic correlation contribution is already being considered, since the nondynamical component is almost absent in this conformer. For this reason, the values of columns 1 and 2 that correspond to GVB calculations should be considered as an upper bound for the exact values. In columns 4 and 5 of Table 6 we show the automerization energy barriers calculated as

$$\Delta E = E_{D_{4h}}(\mathrm{GVB}) - E_{D_{2h}}(\mathrm{HF}) \ . \tag{61}$$

Although small differences can be seen from functional to functional, these values are very close to the exact ones. The last column shows the effect to take the basis set limit by extrapolating to a cc-pV∞Z base, following the scheme proposed in Ref. [59]. The results achieved in this example show again that the adequate use of methods employing correlation energy functionals is able to give as accurate values as those that use much more elaborate and computationally demanding ones.

3.4 Excited states

The development of correlation energy functionals in the framework of DFT presents serious conceptual difficulties that have not yet been solved. The Hohenberg–Kohn (HK) theorem, which supports DFT, is a ground-state theorem and does not guarantee the existence of a universal variational density functional for the energy of the rest of the electronic states. Moreover, it is widely accepted that if such a functional exists, it would be dependent, not only on the density of the corresponding excited state, but it should also include a dependence on the density of the ground state [60,61]. Although there are interesting works about DFT on excited states [21, 60, 61, 62, 63, 64, 65, 66], the limitations mentioned earlier, as well as the relatively short trajectory of DFT in quantum chemistry, explain the scarce use of energy functionals (in particular, correlation energy functionals) when calculating the properties of excited states of atoms and molecules.

Table 7. UHF + correlation excitation energies, (eV) for the lowest state of each multiplicity, and the average of the absolute error, $\langle|\varepsilon|\rangle$

	UHF	VWN-Sic	B88	CS	MSF	MPJ	Exp.
Helium							
$^{3}S \leftarrow {}^{1}S$	18.711	20.304	19.733	19.842	19.793	19.855	19.83
Beryllium							
$^{3}P^{0} \leftarrow {}^{1}S$	1.618	2.540	2.260	2.287	2.421	2.326	2.73
Boron							
$^{4}P \leftarrow {}^{2}P$	2.081	3.562	3.162	2.975	3.471	3.432	3.58
Carbon							
$^{1}D \leftarrow {}^{3}P$	2.280	1.769	1.951	1.874	1.685	1.687	1.26
$^{5}S \leftarrow {}^{3}P$	2.435	4.469	4.022	3.539	4.403	4.477	4.19
Nitrogen							
$^{2}D \leftarrow {}^{4}S$	3.723	2.979	3.307	3.204	2.816	2.800	2.39
Oxygen							
$^{1}D^{0} \leftarrow {}^{3}P$	3.295	2.777	2.995	2.933	2.640	2.627	1.97
$\langle\lvert\varepsilon\rvert\rangle$	1.31	0.41	0.54	0.59	0.31	0.34	

Correlation energy functionals derived from the CF approach do not depend on any restrictive hypothesis regarding the nature of the electronic state and can be applied without limitation to calculate the correlation energy of any electronic state.

In Ref. [24] the correlation energies for several states for some atoms of the first row in a post-SCF procedure were calculated. The complete-active-space (CAS)–MCSCF and the HF (for the lowest state of each multiplicity) wave functions were employed. The correlation density functional modified to take into account the explicit dependence on $\rho_2(\mathbf{r})$ through Eq. (55) was used with the CAS–MCSCF wave functions.

The results are shown in Tables 7 and 8. An error due to the basis set incompleteness can be implicit in some excitation energies of these tables mainly due to the importance of the diffuse basis functions. For instance, addition of a p function with an exponent of 0.008 lowers the energy of the ^{3}P and ^{1}P states of He by 5.5 and 8.5 mhartree, respectively.

The HF excitation energies as well as those obtained from the former by adding the correlation energy from functionals described earlier in a post-SCF fashion are listed in Table 7. The HF method provides poor estimates of the excitation energies, which are largely improved when the dynamic correlation energy is included. As an example, in Table 8 the excitation energies corresponding to a wide range of electronic states for the C atom taken from Ref. [24] are shown. Apart from small deviations in some specific cases, the results represent excellent approximations to the exact values. We can check that inclusion of a MC wave function improves

Table 8. Excitation and splitting energies (eV) for the carbon atom with MCSCF + correlation energies, and the average of the absolute error $\langle|\varepsilon|\rangle$

Transition	MCSCF	VWN-Sic	B88	VWNm	B88m	CS	MSF	MPJ	Exp.
$^1D^0 \leftarrow g^3P$	1.574	1.082	1.179	1.166	1.373	1.228	0.988	0.994	1.26
$^1S \leftarrow g^3P$	2.602	2.132	2.153	1.966	1.989	1.933	1.393	1.424	2.69
$^5S \leftarrow g^3P$	2.905	4.942	4.497	4.775	4.333	3.865	4.683	4.758	4.19
$^3D \leftarrow g^3P$	8.480	8.630	8.555	8.669	8.661	8.392	8.458	8.478	7.95
$^3P \leftarrow g^3P$	10.021	10.242	10.163	9.817	9.733	9.594	9.406	9.440	8.96
$^1D \leftarrow g^3P$	14.595	14.178	14.083	14.045	13.944	13.572	13.389	13.412	12.14
$^3S \leftarrow g^3P$	15.344	15.373	15.182	14.838	14.825	14.535	14.613	14.626	13.13
$^1P \leftarrow g^3P$	16.060	15.662	15.577	15.498	15.414	14.779	14.410	14.445	14.87
$^3D \leftarrow {}^5S$	5.574	3.688	4.058	3.894	4.328	4.526	3.775	3.721	3.76
$^3P \leftarrow {}^5S$	7.116	5.300	5.666	5.042	5.400	5.729	4.723	4.682	5.15
$^1D \leftarrow {}^5S$	11.690	9.236	9.586	9.270	9.610	9.707	8.707	8.654	7.98
$^3S \leftarrow {}^5S$	12.438	10.431	10.685	10.063	10.492	10.670	9.931	9.868	8.93
$^1P \leftarrow {}^5S$	13.155	10.720	11.080	10.723	11.081	10.914	9.727	9.688	10.68
$\langle|\varepsilon|\rangle$	1.75	0.90	0.93	0.77	0.85	0.78	0.72	0.72	

Table 9. First IP, EA and polarizabilities, α, of He–Ar atoms, using a SCF procedure

	IP			EA			α		
	Exact	ROHF	MPJ	Exact	ROHF	MPJ	Exact	ROHF	MPJ
2	24.59	23.46	24.60	–	< 0	< 0	0.21	0.19	0.19
3	5.39	5.34	5.66	0.62	−0.13	0.42	24.30	25.08	24.61
4	9.32	8.04	8.96	–	< 0	< 0	5.60	6.77	6.57
5	8.30	7.93	8.50	0.28	−0.27	0.05	3.03	3.26	3.07
6	11.26	10.79	11.31	1.27	0.55	0.88	1.76	1.78	1.67
7	14.53	13.97	14.43	–	< 0	< 0	1.10	1.08	1.02
8	13.62	11.98	13.68	1.47	−0.54	0.76	0.80	0.70	0.67
9	17.42	15.71	17.27	3.41	1.31	2.52	0.56	0.48	0.46
10	21.56	19.87	21.28	–	< 0	< 0	0.40	0.32	0.32
11	5.14	4.95	5.22	0.55	−0.12	0.48	23.60	28.12	26.53
12	7.65	6.61	7.53	–	< 0	< 0	10.60	12.06	11.48
13	5.99	5.50	5.99	0.45	0.04	0.32	8.34	9.27	8.65
14	8.15	7.66	8.11	1.40	0.96	1.26	5.38	5.71	5.44
15	10.49	10.18	10.46	0.76	−0.46	0.77	3.63	3.76	3.62
16	10.36	9.09	10.62	2.09	0.90	2.07	2.90	2.83	2.70
17	12.97	11.79	13.20	3.64	2.53	3.63	2.18	2.10	2.02
18	15.76	14.74	16.05	–	< 0	< 0	1.64	1.59	1.54
ϵ		7.27	1.50		108.10	24.81		9.1	8.2

noticeably the results obtained with a HF plus correlation calculation.

Therefore, the combination of a MCSCF calculation with a density functional modified by Eq. (55) or a CF functional seems to be a method applicable to both excited and ground states. This finding is of particular interest for DFT functionals, because it suggests that these functionals which, according to the HK theorem have been designed to study ground states, are also applicable to excited states.

4 SCF calculations for atoms and diatomic molecules

In Refs. [67,68] extensive self-consistent calculations by using a KS-type scheme including both the exact exchange potential and a correlation potential obtained as the functional derivative of the MPJ functionals were made. The ground states of atoms and small molecules incorporating these correlation potentials were calculated using two types of wave functions: either a single Slater determinant or a GVB-PP wave function. The latter is needed for the correct description of the whole PEC of the molecules studied.

4.1 Atomic properties

Some of the results for several atomic properties obtained from ROHF calculations are shown in Table 9. The IP and EA were calculated by using Eqs. (45) and (46), while the atomic polarizabilities refer to the average polarizability or isotropic term of the polarizability tensor [67]:

$$\bar{\alpha} = \frac{1}{3}(2\alpha_{xx} + \alpha_{yy}) \ , \tag{62}$$

where

$$\alpha_{ij} = \left(\frac{\delta \mu_i}{\delta F_j}\right)_{F=0} \ , \tag{63}$$

while μ_i is the permanent dipole moment and F is the intensity of the applied electric field.

In a previous section we discussed the effect of the basis set quality on the IP and EA results calculated in a post-SCF fashion. The calculation of the atomic polarizabilities requires large basis sets with inclusion of diffuse functions. The ANO-TZ basis set [26,27] is adequate for this purpose.

The SCF IP and EA from Table 9 are very similar to those of Tables 1 and 2 from post-SCF calculations. The differences between the mean relative errors of both sets are only of 0.18 and 6.33, respectively, favoring slightly the SCF results. Both sets of values improve markedly on the HF ones. The values of the polarizabilities of Table 9 are slightly better than those from ROHF calculations, being the highest improvements for the atoms of the second row.

4.2 Molecular properties

4.2.1 One-determinant calculations

Regarding the SCF results for small molecules we list in Table 10 the dissociation energies, vibrational frequencies, equilibrium distances and dipole moments calculated using a single Slater determinant to approximate the wave function of homonuclear and heteronuclear diatomic molecules [68]. The use of just one Slater determinant does not allow an adequate description of the PEC at dissociation distances. For this reason, the dissociation energies were calculated as the difference between the energy of the molecule at equilibrium distance and the sum of the energies of the isolated atoms.

These results reaffirm the conclusions drawn from the atomic SCF calculations, namely:

- The equilibrium distances, vibrational frequencies and dipole moments are slightly improved when the correlation energy is taken into account (the MPJ functional gives the best values).
- The dissociation energies are largely improved when the correlation energy is considered. For example, the MPJ functional gives an average relative error of 15.9% versus 59.4% for the HF calculation.

The atomization energies of four polyatomic molecules taken from Ref. [68] are shown in Table 11. The large improvement of the correlated SCF results with respect to the HF method is immediately apparent, with the best results achieved by the MPJ functional. We note in passing that the atomization energy for the ozone molecule is poorly described, because the ground state of C_{2v} symmetry has a large portion of birradical character. Therefore, at least two Slater determinants are needed for a correct description of the molecule.

4.2.2 Many-determinant calculations

We end this section by stressing the influence of the many-determinant character of the wave function in the SCF determination of PECs, and by analyzing the effect of including or not the correlation contribution to a many-determinant SCF procedure. We start the discussion by noting that, in general, more than one Slater determinant is needed for the correct determination of the PEC at all distances in diatomic molecules. To simplify things, we will only focus on molecules where

Table 10. Molecular properties from correlated SCF calculations. (R_e in atomic units, D_e in electron volts, ω_e in reciporcal centimeters and $|\mu|$ in debyes)

	H_2	Li_2	B_2	C_2	N_2	O_2	F_2	LiH	BeH	HB	HF	HCl	ε
Exact													
R_e[a]	1.401	5.051	3.003	2.347	2.073	2.282	2.679	3.015	2.538	2.336	1.733	2.409	
D_e[a]	4.75	1.14	3.00	6.36	9.91	5.21	1.66	2.52	2.20	3.58	6.12	4.62	
ω_e[a]	4400	351	1051	1855	2358	1580	892	1406	2061	2368	4139	2991	
$\|\mu\|$[b]								5.83	0.17	1.27	1.82	1.08	
ROHF													
R_e	1.390	5.263	3.098	2.351	2.022	2.176	2.516	3.037	2.535	2.314	1.693	2.399	2.2
D_e	3.62	0.17	0.86	0.65	4.96	1.10	−1.49	1.47	2.16	2.74	4.18	3.41	59.4
ω_e	4594	337	944	1911	2740	2030	1212	1431	2136	2476	4513	3148	10.5
$\|\mu\|$								6.03	0.29	1.72	1.98	1.45	30.4
ROHF-VWN													
R_e	1.363	5.107	3.041	2.321	2.005	2.154	2.483	2.969	2.492	2.271	1.676	2.371	2.8
D_e	6.21	0.93	1.15	2.04	7.34	2.25	−0.89	3.30	3.30	4.38	5.95	5.02	44.1
ω_e	4773	368	1006	1985	2804	2093	1263	1507	2218	2599	4637	3251	13.6
$\|\mu\|$								6.01	0.29	1.77	1.99	1.43	31.0
ROHF-LYP													
R_e	1.379	5.100	3.042	2.324	2.008	2.156	2.479	2.976	2.503	2.284	1.682	2.380	2.5
D_e	4.66	0.89	1.32	2.32	7.65	2.66	−0.57	2.43	2.51	3.60	5.30	4.37	32.3
ω_e	4672	364	1006	1986	2797	2093	1277	1497	2192	2562	4597	3222	12.9
$\|\mu\|$								5.93	0.28	1.76	1.99	1.47	30.0
ROHF-MPJ													
R_e	1.377	5.156	3.054	2.328	2.012	2.163	2.493	2.989	2.502	2.281	1.682	2.375	2.1
De	4.57	1.44	2.17	3.62	9.50	4.32	1.39	2.61	2.80	3.92	5.59	4.76	15.9
ω_e	4689	357	993	1976	2788	2076	1253	1485	2200	2578	4604	3246	12.6
$\|\mu\|$								6.02	0.27	1.76	1.98	1.43	28.4

[a] The exact values are taken from Refs. [79, 80], except for HCl [81]

[b] The exact values are taken from Ref. [82], except for the CEPA values of HBe [83]

Table 11. Atomization energies (kcal mol^{-1}) using correlated SCF calculations

	H_2O	NH_3	H_2O_2	O^3
HF	155.1	198.4	138.3	– 8.9
HF-VWN	237.4	323.4	238.4	1.6
HF-LYP	207.1	277.6	215.0	17.8
HF-MPJ	221.9	300.7	273.5	111.9
Exp.	234.5	300.9	271.9	148.8

two determinants are sufficient to obtain a correct description at any distance. In this case the minimization of the energy is done through an iterative procedure where each step consists of two phases: in the first one we optimize the molecular orbitals while keeping fixed the amplitudes of each determinant entering the wave function; in the second one we optimize the previously mentioned amplitudes without changing the molecular orbitals. Although a more elaborate description of the procedure may be found in Ref. [22], we give here a brief outline:

- In a first step the following three sets of differential equations are solved:

  $$H_{\mathrm{c}}^{\mathrm{ef}}\psi_i = \epsilon_i\psi_i \ , \tag{64}$$

  $$H_{\mathrm{b}}^{\mathrm{ef}}\psi_b = \epsilon_b\psi_b \ , \tag{65}$$

  $$H_{\mathrm{a}}^{\mathrm{ef}}\psi_a = \epsilon_a\psi_a \ , \tag{66}$$

  where $H_{\mathrm{c}}^{\mathrm{ef}}$, $H_{\mathrm{b}}^{\mathrm{ef}}$ and $H_{\mathrm{a}}^{\mathrm{ef}}$ represent the effective one-electron operators of the core shell, the bonding and the antibonding orbital, respectively, while i runs through the number of orbitals of the core shell. Each of these operators is built by adding the corresponding correlation potential to the "noncorrelated" operator.[1] The way this correlation potential is obtained is described in Ref. [22].
- In the second phase the probability amplitude of each Slater determinant entering the MC wave function is optimized, as in a CI calculation.

The results obtained from MCSCF calculations with and without correlation included are shown in Table 12. We only report on the MPJ functional because it is the one that yields the best results. The behavior of the PECs and spectroscopic properties upon the inclusion of correlation energy functionals was discussed in Sect. 3, and the main conclusions apply equally well here. Namely, the inclusion of the correlation functionals in the MC calculation

- Decreases the GVB equilibrium distances, improving its values. Note that the same lowering occurs when adding the correlation functional to HF.
- Increases the vibrational frequencies, which also improves the results.
- Increases the dissociation energy of the GVB case, largely improving the values.

Table 12. Equilibrium distances (au), vibrational frequencies (cm^{-1}) and dissociation energies (eV) for some diatomic molecules

	H_2	F_2	LiH	HF
GVB				
R_{e}	1.426	2.777	3.088	1.729
D_{e}	4.14	0.72	1.93	4.98
ω_{e}	4226	691	1300	4132
GVB + MPJ				
R_{e}	1.400	2.690	3.011	1.706
D_{e}	4.93	1.15	2.70	6.00
ω_{e}	4429	817	1384	4331
GVB-MPJ(SCF)				
R_{e}	1.400	2.690	3.011	1.707
D_{e}	4.93	1.15	2.73	6.02
ω_{e}	4422	823	1414	4327

The differences found between SCF and post-SCF calculations on the many-determinant scheme are also very little, although the values improve slightly when going from the post-SCF to the SCF calculations. For example, the vibrational frequencies are modified by the order of several reciprocal centimeters (LiH has the higher difference of 30 cm^{-1}).

5 Size-consistency

Size-consistency is an important property in molecular calculations. We say that a computational method is size-consistent if the energy of the compound system AB tends to the energy of the component subsystems A and B at infinite separation,

$$\lim_{R_{\mathrm{AB}}\to\infty} E_{\mathrm{AB}} = E_{\mathrm{A}} + E_{\mathrm{B}} \ . \tag{67}$$

Size-consistency is part of the more general concept size-extensivity. A computational method is size-extensive if the calculation of the energy properties of a system composed of several noninteracting subsystems gives the sum of the properties for every isolated subsystem,

$$E(S_1 + S_2 + \cdots + S_m) = E(S_1) + E(S_2) + \cdots + E(S_m) \ . \tag{68}$$

Some of the more common quantum chemistry methods do not satisfy these properties of size-extensivity or size-consistency. For example, the truncated CI methods are not size-extensive. This fact can be proved by the analysis of the excitations using a diagrammatic technique. The CI method is size-extensive only when it satisfy Wick's sum where all the unlinked diagrams are adequately compensated.

Some simple theoretical methods are size-consistent, (the HF method and the GVB-PP method are two examples of these methods). Most of the correlation energy functionals are size-consistent. When a correlation energy functional is applied together with a size-consistent wave function (in post-SCF or SCF) the results of this calculation are size-consistent. The conventional DFT correlation energy functionals are

---

[1] With the word noncorrelated we mean that the contribution of the correlation energy functional is absent.

size-consistent because they do not depend on the number of electrons of the system. The CS functional is also size-consistent. However MSF and MPJ functionals depend explicitly on the number of electrons of the system and are not size-consistent, although the exact functional of DFT must be so, because according to Lieb [69] it depends on N.

Recently, a method was proposed to solve the problem of size-consistency for the MSF and MPJ functionals [23]. In this method the number of electrons N of the system is replaced by an effective number of electrons $\tilde{N}(\mathbf{r})$. The number of electrons of a neutral system satisfies the following equation:

$$N = \sum_{i=1}^{M} Z_i \ , \tag{69}$$

where Z_i is the atomic number of atom i and M is the number of atoms of the system.

The Z_i are replaced by an effective number that depends on the distance of the point where we are calculating the effective number of electrons ($\mathbf{r}$) and the position of the nucleus ($\mathbf{R}_i$). The expression for this function proposed in Ref. [23] is

$$\tilde{N}(\mathbf{r}) = \sum_{i=1}^{M} Z_i \exp\left[-\left(\frac{\mathbf{r} - \mathbf{R}_i{}^2}{\alpha}\right)\right] \ , \tag{70}$$

where α is an adjustable parameter. This effective number of electrons satisfies

$$\lim_{\alpha\to\infty} \tilde{N}(\mathbf{r}) = N. \tag{71}$$

So the effective number of electrons tends toward the total number of electrons in the limit of large screening radius.

This definition of the effective number of electrons is not the only one possible; however, it gives very good results on the tests where it was applied. For example, the correlation energy for the Be dimer at internuclear distance of 20 Å with a 6-311G** basis set is −0.230 au for the MPJ functional. The sum of the correlation energy of two Be atoms with the MPJ functional is −0.189 au, showing the importance of the size-consistency. When we introduced the effective number of electrons the same calculations give −0.189 hartree for the molecule at 20 Å and for the two isolated atoms, so the size-consistency problem has been solved.

The PEC of the fluorine molecule is shown in Fig. 5 using a GVB-PP wave function together the CS, the MPJ, and the MPJ corrected by the effective number of electron functionals. The PEC shows that the inclusion of Eq.(70) has solved satisfactorily the lack of size-consistency of the original MPJ functional.

6 Concluding remarks

An overview on two-body functionals for the correlation energy, obtained within the CF approach has been made. Its applications to atomic, molecular properties as well chemical reactivity have been discussed and compared with the results of a wide variety of correlation energy functionals from DFT.

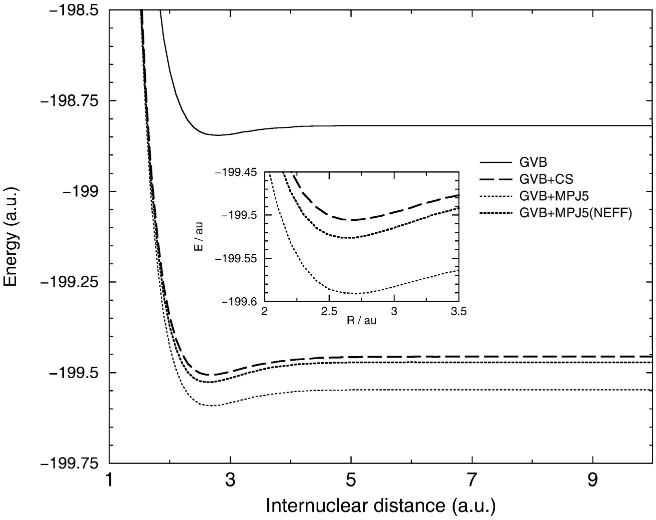

Fig. 5. Post-SCF potential energy curves of F_2 molecule. In a.u.

Properties such as IP, EA and polarizabilities of atoms, equilibrium bond lengths, vibrational frequencies, dissociation energies, and the slope of the PEC of diatomic molecules were analyzed. Two kinds of chemical reactions were considered: a set of reactions implying changes in the ionicity of the reactants and a typical organic isomerization reaction in which the evolution of π bonds is the key point; in both kinds of reactions the electron correlation plays an important role but in a very different fashion.

The conclusions are basically the same for all the properties discussed. If the one-Slater-determinant wave function is adequate for a qualitatively correct picture of the system under study, both sets of functionals, GGA DFT and CF, are good tools to include the correlation energy, providing very satisfactory results (the CF ones giving slightly better results). When a many-determinant wave function is needed for an acceptable picture of the electron cloud, the correlation energy functionals pertaining to the CF class maintain their good performances, but the DFT class does not. Anyway, if the spin components of the density are modified, in the sense that they depend now on the two-body density matrix through the on-top two-body density, the DFT functionals work adequately without modifying their original expressions.

Unfortunately, dynamic and nondynamic (short-range and long-range) correlation energy components are somewhat artificial concepts and are not completely separable.Therefore, the results of applying correlation energy functionals must show, to some extent, a double count of the correlation energy. This fact appears in both sets of functionals analyzed but to a much more extent in the DFT ones. CF functionals show an acceptable accommodation to the wave function, reducing in a reasonable fashion the amount of correlation energy which they provide when the quality of the wave function increases. Other attempts have been made to solve this double count of the correlation energy [70, 71, 72, 73, 74, 75]; however, a definitive solution has not yet been reached and remains a difficult task to be done in the future.

CF and DFT correlation energy functionals were applied, in a post-SCF scheme, to the calculation of excited-state energies of atoms. There are not conceptual restrictions to apply the CF functionals to excited-state calculations, but DFT functionals are related to the HK theorem, which applies only to the ground-state energy of each symmetry. There are no significant differences between the results of both sets of functionals, (DFT and CF), both being very good.

Self-consistent calculations, using an effective Hamiltonian with the correlation energy potential obtained as the functional derivative of a correlation energy functional, provide slightly better results than those obtained in post-SCF calculations. Nevertheless, the differences are so small that in many cases the effort required in the SCF calculation would not be justified compared to the post-SCF results.

In the KS hypothesis there is an auxiliary system described by one Slater determinant that provides the density of the exact system. Once the exact density is obtained the calculation of the energy follows from placing it into the energy density functional. However, the one-determinant KS calculations show the same behavior as the HF ones. When a departure from the one determinant solves the deficiencies of the HF model, the same wave function suffices for good results by using any of the correlation DFT functionals, without changing their expressions, only by using Eqs. (54) and (55). This fact indicates that the one-determinant hypothesis is a restriction to be removed from KS theory. Moreover, it must be stressed that for a KS theory workable in any circumstances, the on-top density is needed and not only the exact density. This is a very interesting fact pointed out in the literature [44, 45, 76] which deserves further and deeper analysis.

The MSF and MPJ functionals were obtained by using a Gaussian sum to approximate the angle-averaged two-body density; this fact, together with the use of the hierarchy between the two-body and one-body densities as a constraint, leads to an energy functional having a particular dependence on the number of electrons. An important consequence for these functionals is that they are not size-extensive. We have shown that this limitation can be removed in an approximate and satisfactory way by introducing the intensive modified electron number.

Acknowledgement. This work has been done under the support of the Spain DGICYT, project n^0 BQU2001-0883.

References

1. Parr RG, Yang W (1989) Density-functional theory of atoms and molecules. Oxford University Press, New York
2. Nesbet RK, Colle R (1999) Phys Rev A 61: 012503
3. Colle R, Salvetti O (1975) Theor Chim Acta 37: 329
4. Lee C, Yang W, Parr RG (1988) Phys Rev B 37: 785
5. Hylleraas EA (1928) Z Phys 48: 469
6. Egil V, Hylleraas A (1929) Z Phys 54: 347
7. Wigner E (1934) Phys Rev 46: 1002
8. Colle R, Salvetti O (1979) Theor Chim Acta 53: 55
9. Colle R, Salvetti O (1983) J Chem Phys 79: 1404
10. Colle R, Salvetti O (1990) J Chem Phys 93: 534
11. Singh R, Massa L, Sahni V (1999) Phys Rev A 60: 4135
12. Caratzoulas S, Knowles PJ (2000) Mol Phys 98: 1811
13. Tao J, Gori-Giorgi P, Perdew JP, McWeeny R (2001) Phys Rev A 63: 032513
14. Moscardó F, Pérez-Jiménez AJ (1997) Int J Quantum Chem 61: 313
15. Moscardó F, San-Fabián E (1991) Int J Quantum Chem 40: 23
16. Coleman AJ (1973) Rep Math Phys 4: 113
17. Harriman JE (1984) Phys Rev A 30: 19
18. Berkowitz M (1986) Chem Phys Lett 129: 486
19. Lee C, Parr RG (1987) Phys Rev A 35: 2377
20. Stoll H, Pavlidou CME, Preuss H (1978) Theor Chim Acta 49: 143
21. Oliveira LN, Gross EKU, Kohn W (1988) Phys Rev Lett 60: 2430
22. Moscardó F et al (1998) J Phys Chem A 102: 10900
23. Pérez-Jiménez AJ et al (2001) J Chem Phys 114: 2022
24. San-Fabián E, Pastor-Abia L (2003) Int J Quantum Chem 91: 451
25. San-Fabián E, Moscardó F, Pérez-Jordá JM (1994) Int J Quantum Chem 52: 1027
26. Widmark PO, Malmqvist PA, Roos BO (1990) Theor Chim Acta 77: 291
27. Widmark PO, Persson BJ, Roos BO (1991) Theor Chim Acta 79: 419
28. San-Fabián E, Moscardó F (1984) J Chem Phys 81: 4008
29. Vosko SH, Wilk L, Nusair M (1980) Can J Phys 58: 1200
30. Perdew JP (1986) Phys Rev B 33: 8822
31. Davidson ER et al (1991) Phys Rev A 44: 7071
32. Chakravorty SJ et al (1993) Phys Rev A 47: 3649
33. Hotop H, Lineberger WC (1985) J Phys Chem Ref Data 14: 731
34. de la Vega JMG (1995) Phys Rev A 51: 2616
35. Fraga S, Saxena K, Karwowski J (1975) Hartree-Fock atomic data. University of Alberta Press, Edmonton
36. Fraga S, Karwowski J, Saxena K (1979) Physical sciences data 5: Handbook of atomic data. Elsevier, Amsterdam
37. Goddard WA III, Ladner RC (1971) J Am Chem Soc 93: 6750
38. Ladner RC, Goddard WA III (1969) J Chem Phys 51: 1073
39. Hunt W, Hay PJ, Goddard WA III (1972) J Chem Phys 57: 738
40. Pérez-Jordá JM, San-Fabián E, Moscardó F (1992) Phys Rev A 45: 4407
41. Pople JA (1977) In: Schaefer HF III (ed) Applications of electronic structure theory, Vol. 4. Plenum, New York pp 1–27
42. San-Fabián E et al (1992) J Mol Struct (THEOCHEM) 254: 1
43. Kolos W, Wolniewicz L (1965) J Chem Phys 43: 2429
44. Moscardó F, San-Fabián E (1991) Phys Rev A 44: 1549
45. Becke AD, Savin A, Stoll H (1995) Theor Chim Act 91: 147
46. Sancho-García JC, Moscardó F (2003) J Chem Phys 118: 1054
47. Mok DKW, Neumann R, Handy NC (1996) J Phys Chem 100: 6225
48. Moscardó F, Pérez-Jiménez AJ (1998) J Mol Struct (THEOCHEM) 426: 47
49. Illas JRF, Bagus PS, Gonzalez M (1991) J Chem Phys 94: 3774
50. Becke AD (1988) J Chem Phys 88: 1053
51. Kohn W, Sham LJ (1965) Phys Rev A 140: 1133
52. Becke AD (1988) Phys Rev A 38: 3098
53. Becke AD (1993) J Chem Phys 98: 5648
54. Arnold B, Michl J (1989) In: Platz M (ed) Kinetics and spectroscopy of carbenes and diradicals. Plenum, New York
55. Cársky P et al (1988) J Chem Phys 89: 3008
56. Balková A, Barlett RJ (1994) J Chem Phys 101: 8972
57. Sancho-García JC, Pittner J, Cársky P, Hubac I (2000) J Chem Phys 112: 8785
58. Sancho-García JC, Pérez-Jiménez AJ, Moscardó F (2000) Chem Phys Lett 317: 245
59. Halkier A et al (1998) Chem Phys Lett 286: 243
60. Görling A (1996) Phys Rev A 54: 3912

61. Levy M, Nagy A (1999) Phys Rev Lett 83: 4361
62. Kohn W (1986) Phys Rev Lett 56: 2219
63. Gunnarsson O, Lundqvist BI (1976) Phys Rev B 13: 4274
64. Theophilou AK (1979) J Phys C 12: 5419
65. Gross EKU, Oliveira LN, Kohn W (1988) Phys Rev A 37: 2805
66. Oliveira LN, Gross EKU, Kohn W (1988) Phys Rev A 37: 2809
67. Moscardó F, Pérez-Jiménez AJ (1998) J Comp Chem 19: 1887
68. Moscardó F, Pérez-Jiménez AJ, Cjuno JA (1998) J Comput Chem 19: 1899
69. Lieb EH (1983) Int J Quantum Chem 24: 243
70. Malcolm NOJ, McDouall JW (1994) J Phys Chem 98: 12579
71. Malcolm NOJ, McDouall JJW (1996) J Phys Chem 100: 10131
72. Malcolm NOJ, McDouall JJW (1997) J Phys Chem 101: 8119
73. Malcom NOJ, McDouall JW (1998) Chem Phys Lett 282: 121
74. Miehlich B, Stoll H, Savin A (1997) Mol Phys 91: 527
75. Gräfenstein J, Cremer D (2000) Chem Phys Lett 316: 569
76. Perdew J, Savin A, Burke K (1995) Phys Rev A 51: 4531
77. Gerard-Ain M (1980) J Phys B 13: L131
78. Helm H, Cosby PC, Huestin DL (1984) Phys Rev A 30: 851
79. Lie GC, Clementi E (1974) J Chem Phys 60: 1288
80. Lie GC, Clementi E (1974) J Chem Phys 60: 1275
81. Woon DE, Dunning TH Jr (1993) J Chem Phys 99: 1914
82. Hehre W, Radom L, Schleyer P, Pople J (1986) Ab initio molecular orbital theory. Wiley, New York
83. Meyer W, Rosmus P (1975) J Chem Phys 63: 2356